Flow Turbulence Combust (2012) 89:295–309
DOI 10.1007/s10494-011-9371-y

Subgrid Linear Eddy Mixing and Combustion Modelling of a Turbulent Nonpremixed Piloted Jet Flame

José Salvador Ochoa · Alberto Sánchez-Insa · Norberto Fueyo

Received: 17 September 2010 / Accepted: 8 September 2011 / Published online: 28 October 2011

Abstract A linear eddy model for subgrid mixing and combustion has been coupled to a large eddy simulation of the turbulent nonpremixed piloted jet flame (Sandia Flame D). For the combustion reaction, simplified, single-step, irreversible, Arrhenius kinetics are used. The large scale and the subgrid structure of the flow are compared with experimental observations and, where appropriate, with a flamelet model of the flame. The main objective of this work is to demonstrate the feasibility of the LES-LEM approach for determining the structure of the subgrid scalar dissipation rate and the turbulence-chemistry interactions. The results for the large- and subgrid-scale structure of the flow show a reasonable agreement with the experimental observations.

Keywords LES · LEM · Nonpremixed flame · Scalar dissipation · Subgrid modelling

1 Introduction

Despite the progressive increase in computing power, Direct Numerical Simulation (DNS) of turbulent combustion is a prohibitive task in most practical situations due to the resolution requirements for solving the wide range of scales involved in turbulent reacting flows. Large Eddy Simulation (LES) has emerged as alternative for simulating the complex large-scale flow structures, although small-scale mixing and combustion processes need to be modelled, frequently by resort to approaches adapted from widely used models of Reynolds-Averaged models (RANS) [1]. The Linear Eddy Model (LEM) was originally developed by Kerstein [2, 3] to solve accurately the turbulent mixing, diffusion and chemical reactions in a one-dimensional domain over the whole range of scales in the scalar field. An approach that combines

J. S. Ochoa · A. Sánchez-Insa · N. Fueyo (✉)
Fluid Mechanics Group, University of Zaragoza and LITEC (CSIC),
María de Luna 3, 50018, Zaragoza, Spain
e-mail: Norberto.Fueyo@unizar.es

the features of LEM and LES has been proposed in the past [4] and has been used to study mixing layers [5, 6], premixed [7] and nonpremixed [8] combustion using mainly fast-chemistry assumptions or single-step chemical kinetics. In this work, a subgrid LEM model (called hereafter LES-LEM) is developed to be coupled to the LES solver and predict the evolution of a turbulent nonpremixed flame (Sandia Flame D). The subgrid structure of the scalars is extracted and compared with those provided by experimental observations. The nonpremixed piloted flame D is a well-known benchmark case that has been numerically simulated by many authors, often in the cooperative framework of the International Workshop on Measurements and Computation of Turbulent Nonpremixed Flames (TNF) [9]. In the context of LES, predictions of this flame have been made using CMC (Conditional Moment closure) [10], flamelet approaches assuming steady [11, 12] and unsteady [13–15] state, and Probability Density Function (PDF) methods [16–18]. Despite the abundant literature available for this flame, as far as the authors of this work know, this is the first LEM modelling of the Sandia Flame D. Experimental data consisting of scalar dissipation measurements have been made available in Karpetis and Barlow [19, 20]. These data are an excellent opportunity to validate the LES-LEM modelling of the scalar dissipation and its subgrid-LEM structure. Practically, there is no previous analysis of the feasibility to obtain the scalar dissipation by the LEM model in turbulent flames. Works using LEM as a stand-alone model have shown its ability to reproduce properly statistical features of the scalar fields such as scalar dissipation turbulent mixing layers [21]. One of the main objectives of this work is to demonstrate the feasibility of the LES-LEM approach to determine the structure of the subgrid scalar dissipation rate of the turbulent flame.

A brief background of the main aspects of the LES-LEM approach is given in the next sections followed by a short descriptions of the configuration and the numerical setup of the coupling among models. Then, results are reported and discussed.

2 Mathematical Formulation

The LES-LEM approach follows similar practices as other, more conventional LES: large scales are explicitly captured by the mesh and numerically computed by the filtered transport equations, and subgrid models deal with the unresolved scales. Figure 1 shows schematically the coupling between the transport equations solved by LES and the corresponding variables involved in the LEM solver.

2.1 LES equations

The filtered equations are continuity, momentum and the subgrid kinetic energy, which is used to close the subgrid stresses in the momentum equation through an eddy viscosity model [22]. This set of equations can be written as:

$$\frac{\partial \bar{\rho}}{\partial t} + \frac{\partial \bar{\rho}\tilde{u}_j}{\partial x_j} = 0, \tag{1}$$

$$\frac{\partial \bar{\rho}\tilde{u}_i}{\partial t} + \frac{\partial \bar{\rho}\tilde{u}_i\tilde{u}_j}{\partial x_j} = -\frac{\partial \bar{p}}{\partial x_i} + \frac{\partial}{\partial x_j}\left(\bar{\rho}\bar{\nu}\tilde{S}_{ij}\right) - \frac{\partial \tau^s_{ij}}{\partial x_j}, \tag{2}$$

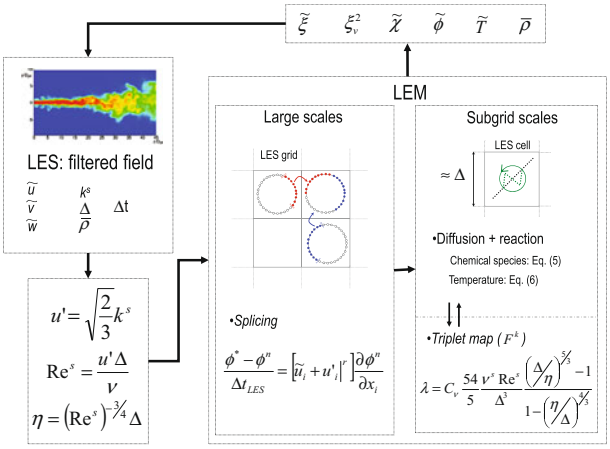

Fig. 1 Schematic representation of the LES-LEM coupling and variables involved in each process

$$\frac{\partial \bar{\rho} k^s}{\partial t} + \frac{\partial \bar{\rho} \tilde{u}_i k^s}{\partial x_i} = -\tau_{ij}^s \frac{\partial \tilde{u}_i}{\partial x_j} - C_\epsilon \frac{\bar{\rho}}{\Delta} \left(k^s\right)^{3/2} + \frac{\partial}{\partial x_i} \left(\bar{\rho} \frac{\nu^s}{\sigma^s} \frac{\partial k^s}{\partial x_i} \right), \tag{3}$$

$$\nu^s = C_\nu \left(k^s\right)^{1/2} \Delta. \tag{4}$$

Here, $\tilde{u}_i$ is the ith (favre filtered) velocity component, $\bar{\rho}$ is the density, $\bar{p}$ is the pressure, k^s is the subgrid turbulent kinetic energy, ν^s is the subgrid eddy turbulent viscosity and Δ is the filter size, equal to $\left(\Delta_x \Delta_y \Delta_z\right)^{1/3}$, where Δ_x, etc., are the local cell spacing. Also, $\tilde{S}_{ij} = \frac{1}{2}\left(\frac{\partial \tilde{u}_j}{\partial x_i} + \frac{\partial \tilde{u}_i}{\partial x_j}\right)$ is the strain rate tensor and $\tau_{ij}^s = -2\bar{\rho}\nu^s \left(\tilde{S}_{ij} - \frac{1}{3}\tilde{S}_{kk}\delta_{ij}\right) + \frac{2}{3}\bar{\rho}k^s\delta_{ij}$ is the subgrid stress tensor. σ^s represents the subgrid Prandtl number, taken as unity, and C_ϵ and C_ν are constants taken as 0.916 and 0.067 respectively [22].

2.2 LEM solver

The LEM solver models both subgrid- and large-scale processes. The velocity field is split into a filtered LES-resolved part $\tilde{u}_i$ and a fluctuation component u_i' which can be in turn composed of an LES-resolved fluctuation $u_i'|^r$ and an unresolved subgrid fluctuation $u_i'|^s$. This general decomposition of the instantaneous velocity field can be written as $u_i = \tilde{u}_i + u_i'|^r + u_i'|^s$ [23, 24].

2.2.1 Subgrid-LEM processes

The physical processes occurring below the LES grid scale such as subgrid turbulent convection, molecular diffusion and chemical reaction are modeled in a one-dimensional domain immersed in each LES cell according to the the conventional

LEM approach in the manner first proposed by Kerstein [2, 3]. A diffusion-reaction equation is used to describe the evolution of any scalar ϕ_i:

$$\rho \frac{\partial \phi_i^k}{\partial t^s} = -\frac{\partial}{\partial s}\left(\rho D_i \frac{\partial \phi_i^k}{\partial s}\right) + F^k + \rho \dot{\omega}_i^k, \tag{5}$$

where the superscript k represents each of the N_{LEM} elements that discretize the subgrid field along the one-dimensional s-coordinate having a total length equal to the LES filter size. Also, ρ is the mixture density, D_i is the scalar diffusivity and $\dot{\omega}^k$ is the mass reaction rate. The number of elements is estimated in such a way that the smallest scale in flow (usually the Kolmogorov scale η) is resolved. F^k stands for the subgrid-scale (turbulent) convection and is modelled by triplet-map stochastic processes [25]. A similar equation can be deduced for the subgrid temperature (T^k) [26]:

$$\rho C_{p,mix}^k \frac{\partial T^k}{\partial t^s} = -\sum_{i=1}^{N_s} \rho C_{p,i}^k D_i^k \frac{\partial \phi_i^k}{\partial s}\frac{\partial T^k}{\partial s} + \frac{\partial}{\partial s}\left(\overline{\kappa}\frac{\partial T^k}{\partial s}\right) - \sum_{i=1}^{N_s} h_i \dot{\omega}_i^k + F^k, \tag{6}$$

where C_p is the specific heat capacity, N_s represents the total number of chemical species, κ is the mixture averaged thermal conductivity, and h_i is the enthalpy of the ith species. Both Eqs. 5 and 6 are time integrated using a time step δt^s imposed by the local subgrid diffusion (or chemistry) scales and determined in this work as [4]:

$$\delta t^s = C_{dif} \frac{(\delta s)^2}{max\,(\nu^s,\, D_i)}, \tag{7}$$

where C_{dif} is a constant, taken, for numerical stability purposes, as 0.25; and δs is the size of the LEM cell. The effect of the subgrid turbulent convection, symbolically represented by the term F^k, is modelled as in the original LEM model by stochastic triplet map events. These events are characterised by three parameters: the frequency of the event per unit length, given by [27],

$$\lambda = C_v \frac{54}{5}\frac{\nu^s Re^s}{\Delta^3}\frac{(\Delta/\eta)^{5/3}-1}{1-(\eta/\Delta)^{4/3}}; \tag{8}$$

a probability density function for the size l of subgrid turbulent eddies,

$$f(l) = \frac{5}{3}\frac{l^{-8/3}}{\eta^{-5/3}-\Delta^{-5/3}} \qquad \eta < l < \Delta \qquad ; \tag{9}$$

and the random position of the event inside the LEM domain. In the above equations, $Re^s = u'\Delta/\nu$ is the subgrid Reynolds number, where $u' = \sqrt{(2/3)k^s}$. From the frequency λ, the time step among triplet-map events can be determined as:

$$\delta t^F = \frac{1}{\lambda \Delta}. \tag{10}$$

For the reaction rate $\dot{\omega}$, the single-step Arrhenius kinetics scheme recently proposed by Fernández-Tarrazo et al. [28] is used. The scheme adjusts the total heat of reaction q and the activation temperature T_a with the equivalence ratio Φ to describe the effect of partial fuel oxidation on the amount of heat release, and to mimic changes in the underlying chemistry in fuel-rich and very lean combustion.

The kinetics considers a single irreversible reaction between a generic hydrocarbon and oxygen:

$$C_n H_m + \left(n + \frac{m}{4}\right) O_2 \longrightarrow nCO_2 + \frac{m}{2} H_2 O + q(\Phi), \tag{11}$$

with a global rate of the form:

$$\omega = Be^{-T_a(\Phi)/T} C_{C_n H_m} C_{O_2}. \tag{12}$$

where $C_{C_n H_m}$ and C_{O_2} are the concentrations of hydrocarbon and oxygen respectively; for methane, $m = 1$ and $n = 4$, and the pre-exponential factor is $B = 6.9 \times 10^{14}$ cm^3/(mol s). The piecewise function for the activation temperature $T_a(\Phi)$ is:

$$\begin{aligned} \Phi \leq 0.64 &: T_a(\Phi)/T_{a0} = 1 + 8.250\,(\Phi - 0.64)^2\,; \\ 0.64 \leq \Phi \leq 1.07 &: T_a(\Phi)/T_{a0} = 1; \\ \Phi \geq 1.07 &: T_a(\Phi)/T_{a0} = 1 + 1.443\,(\Phi - 1.07)^2\,; \end{aligned} \tag{13}$$

where $T_{a0} = 15{,}900$ K. For the heat released, the proposed function is:

$$\begin{aligned} \Phi \leq 1 &: q(\Phi)/q_0 = 1, \\ \Phi \geq 1 &: q(\Phi)/q_0 = 1 - \alpha(\Phi - 1), \end{aligned} \tag{14}$$

where α is a constant that changes by a small amount for different hydrocarbons, being $\alpha = 0.21$ for methane. q_0 is the total heat released per mole of fuel consumed ($q_0 = 802.4$ kJ/mol for methane). Assuming a unity Lewis number, the local equivalence ratio Φ is related to the mixture fraction ξ by the equation:

$$\Phi = \frac{32\left(n + \frac{m}{4}\right)}{12n + m} \frac{Y_{C_n H_m, F}}{Y_{O_2, A}} \frac{\xi}{1 - \xi}, \tag{15}$$

where $Y_{C_n H_m, F}$ and $Y_{O_2, A}$ denote the values of the fuel and oxygen mass fractions in their feed streams.

The subgrid scalar dissipation is calculated on each kth LEM element according to its usual definition as projected onto the subgrid one-dimensional LEM domain as [25]

$$\chi^k = 2D\left(\frac{\partial \xi}{\partial s}\right)^2. \tag{16}$$

At the end of the subgrid-LEM processes, the filtered value of the scalars is obtained by Favre averaging over the one-dimensional domain.

2.2.2 Large-scale LEM processes

The three-dimensional, LES-resolved convection of the scalar is implemented by a transfer of subgrid fluid elements representing the mass fluxes crossing the LES-cell faces. This method, originally called splicing [5], is the algorithm that couples subgrid mixing to large-scale transport. In splicing events, portions of the LEM domains are

transferred to neighbouring grid LES cells. The amount of information transferred across cell faces is calculated as:

$$N_{\text{splice}} = \Delta t_{\text{LES}} \left[\frac{\rho \left(\widetilde{u}_i + u_i'|^r \right) S_{m,i}}{m_{\text{LES}}} \right] N_{\text{LEM}}, \tag{17}$$

where the convective velocity $\left(\widetilde{u}_i + u_i'|^r \right)$ is determined at each cell-face m, $S_{m,i}$ is the area vector of the face, N_{LEM} is the total number of subgrid-LEM elements and m_{LES} is the mass of the LES cell. The LES-resolved fluctuation is assumed to be locally isotropic and may be written as a function of the subgrid turbulent kinetic energy as $u_i'|^r = \sqrt{(2k^s/3)}$. The location of the LEM elements to be transported is chosen randomly as originally proposed in [5], but taking special precautions so that a newly convected element is not overwritten or convected across more than one cell in the same time step. The thermal expansion of the LEM domain is taken into account at every splicing event by weighting the convected LEM elements with the amount of local mass.

3 Configuration and Numerical Setup

Sandia Flame D has been chosen as a test case to validate the LES-LEM approach. The burner consists of a long fuel pipe that delivers a fuel mixture (methane/air, 1:3 vol.) with a stoichiometric mixture fraction of $\xi_{st} = 0.351$ and a Reynolds number of $Re = 22{,}400$ ($U_{\text{jet}} = 49.6$ m/s, $D_{\text{jet}} = 7.2$ mm). The pilot stream ($U_{\text{pil}} = 11.4$ m/s, $D_{\text{pil}} = 18.2$ mm) consists of a coaxial flow with a fully-burned mixture with $\xi_{\text{pil}} = 0.27$. A laminar coflow stream of air surrounds the burner with a speed of 0.9 m/s. More detailed information may be obtained from the TNF website [9].

The governing equations were discretized on a staggered cylindrical grid with $32 \times 60 \times 310$ grid nodes in, respectively, the x, y and z directions. The domain size has a length of $45 D_{\text{jet}}$ and a diameter of $20 D_{\text{jet}}$. The jet and pilot areas have a finer resolution and the grid is uniform in the y-direction in these regions (jet: 10 nodes, pilot: 12 nodes). After these zones and for the rest of the z-direction, the grid lines are smoothly expanded with a expansion ratio close to unity. Grid independence was tested by using finer meshes (up to 560 axial, 90 radial and 64 azimuthal cells) with no significant changes. The final number of LES-grid cells used ($\approx$0.6 M) is smaller than in other reported LES simulations of this flame (see e.g. [11] using flamelets or [17] with PDF-based methods). However, the length of our domain is reduced in axial direction (but it is still long enough to encompass the three locations where scalar dissipation was experimentally monitored, *viz* 7.5, 15, and $30 D_{\text{jet}}$). Thus the grid density is similar to (or even finer than) other LES studies of this flame. Figure 2 shows and estimate of the resolved fraction of the turbulence kinetic energy estimated using Pope's criterion [29] for the turbulence resolution by the grid. This criterion proposes that a grid-adaptive LES should resolve approximately 80% of the kinetic energy. Although the meaning and value of this kind of analysis is a matter of controversy, and its results must be therefore treated with some caution [10], this estimate is commonly presented in the literature (see e.g. [10, 11])). As it can be seen, there are small regions where the resolved fraction is slightly lower ($\approx$75%) than this criterion suggests, and the vast majority of the domain is in the $\geq$80% interval.

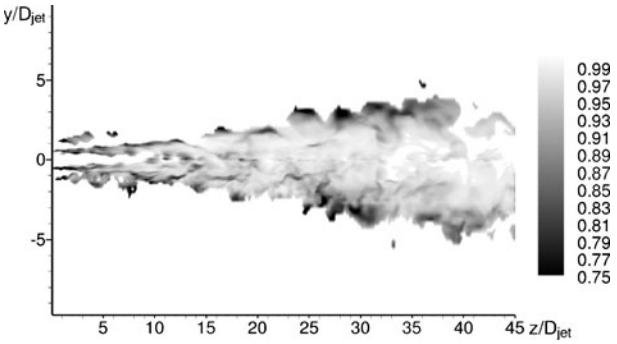

Fig. 2 Resolved part of the turbulent kinetic energy for simulations of Sandia Flame D

At the inflow plane, boundary conditions are generated from the experimental inlet mean profile interpolated onto the grid and by imposing artificial correlated fluctuations. This artificial turbulence satisfies the experimental Reynolds stresses and a length scale according to the method of Klein et al. [30], further refined by Kempf et al. [31]. A simplified mixing-length-scale hypothesis was used to set the length scale as $l = C_l \Delta r$, where C_l is a constant value of $2/3$ [11] and Δr is the distance from the nearest wall.

The LES transport equations are solved by a finite-volume code [32] using an energy-conserving second-order discretization (CDS) scheme for convective terms in LES momentum equations. A Total Variation Diminishing (SMART [33]) was applied for LES scalar transport. Such a flux reconstruction strategy is a common practice in LES of reactive flows [10, 11, 17, 34, 35]. A low-Mach-number formulation is used, whereby the density is updated by the external LEM solver at each time step.

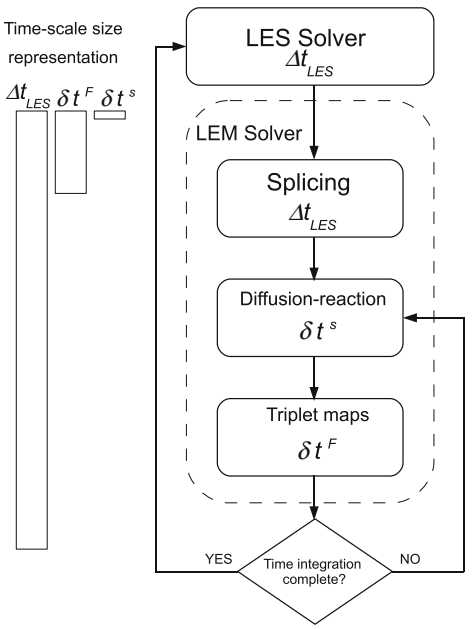

Fig. 3 Schematic flow chart of the LES-LEM time integration

Table 1 Typical CPU time for the LES-FML and LES-LEM simulations

Simulation	Total time	Time step	Relative
LES-FML	33 h 23 min	1 min 3 s	1.00
LES-LEM	103 h 5 min	3 min 20 s	3.18

The dependence of the CFL number is maintained only in the axial direction so that the time step is not drastically reduced. This gives a time step of the order of 10^{-5} s. A fully-implicit third-order Adams-Moulton scheme is used to perform the LES time integration.

After each LES step, the LES solver calls the LEM solver and the splicing algorithm evolves the LEM particles in physical space using filtered velocity and turbulence fields from the LES solver; after this, each subgrid process acts according its time scale (see Fig. 3). A total of 108 subgrid-LEM elements (N_{LEM}) has been used within each LES cell, which resolves the Kolgomorov scale in regions with the highest subgrid turbulence intensity. The filtered-equivalent value of the LEM scalars is obtained by Favre-averaging the subgrid fields when the LEM processes end.

The LES-LEM fields are initialised from the corresponding filtered values obtained from a conventional LES using a steady-state flamelet model (LES-FML) so that the initial transient instabilities are avoided in the computationally expensive LES-LEM simulation. The flamelet libraries are generated using a reduced chemical mechanism for methane-air combustion of 16 species and 35 reactions [36]. In these simulations, the flamelet thermochemical state is a function of the filtered mixture fraction, its subgrid variance and dissipation ($\tilde{\xi}$, ξ_v^2, $\tilde{\chi}$). In this case, both ξ_v^2 and $\tilde{\chi}$ are calculated from a local equilibrium gradient-type model [34] although other options using transport equations were tested with no significant changes [37].

In all cases, statistical results are obtained by collecting data during approximately six residence times (based on the mean inlet velocity at the jet centerline), and once the flow becomes statistically stationary. The required CPU time for the averaging process on a Beowulf cluster using 20 processors (Intel Xeon L5240 3.0GHz Dual-Core) is shown in Table 1. For comparison purposes, the CPU time for LES-FML is also included.

4 Results and Discussion

Time averaged quantities obtained from the LES-LEM approach for Sandia Flame D are compared with experimental data and a steady-state flamelet model below. In Fig. 4, radial profiles of mean and rms axial velocity, mixture fraction and temperature are presented at three axial locations ($z/D_{\mathrm{jet}} = 7.5$, 15 and 30). Both the mean and the rms of these variables are reasonably accurately predicted, sometimes better than with the flamelet model. This be seen also in Fig. 5, especially in the case of the mixture fraction and temperature, where LES-LEM predictions are closer to the experiments than the flamelet ones.

A similar performance can be seen for the mean mass fractions of chemical species CH_4, O_2, H_2O and CO_2 on Fig. 6. In general, these species are well predicted and are in better agreement with the experiments than the ones from flamelet model. At the last location ($z/D_{\mathrm{jet}} = 30$) there are slight discrepancies with an under-prediction

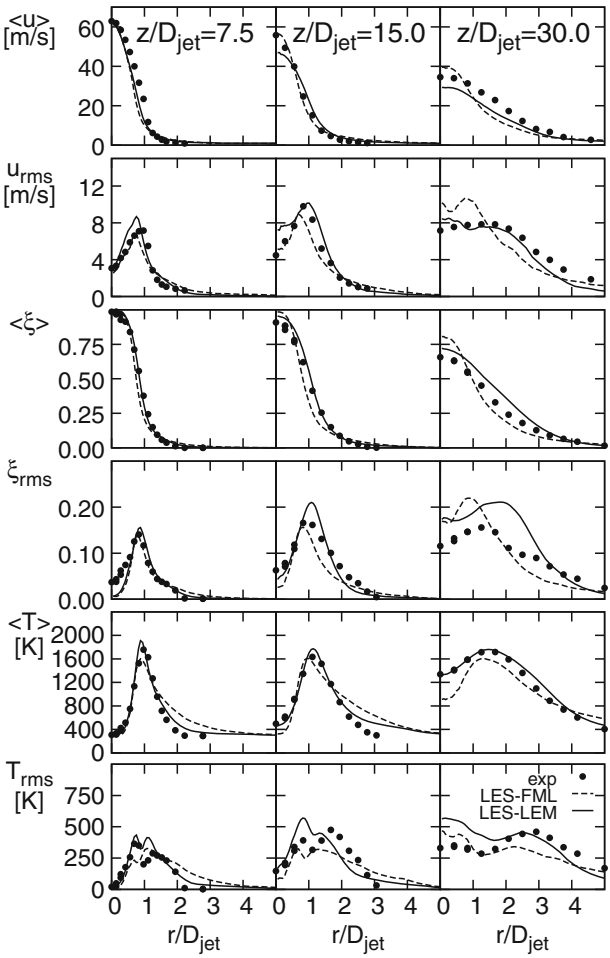

Fig. 4 Radial profiles of averaged (mean and rms) axial velocity, mixture fraction and temperature at several downstream locations

of the consumption of reactants and generation of products that is also presented in flamelets but is more pronounced in LES-LEM. Radial profiles of Reynolds-averaged variance (ξ_v^2) and scalar dissipation (χ) are shown in Fig. 7. In LES-FML, a local equilibrium hypothesis with a gradient-type model was used [34]. Both variance and scalar dissipation exhibit similar trends and values with slightly larger differences in the case of the variance. This indicates that although the LEM modelling of the large-scale convection can potentially result in an unphysical contribution to the scalar dissipation by generating spurious discontinuities in the scalar field, as pointed out by [4, 5], the subgrid events, which have a higher frequency, dampen the role of these discontinuities.

The Reynolds-averaged conditional scalar dissipation rate of the subgrid-LEM mixture fraction is shown in Fig. 8 and is compared with both 1D and 3D measures from Karpetis and Barlow [20]. The computational results are in qualitative agreement with the experimental data although the double-peak structure around the value of stoichiometric mixture fraction ($\xi_{st} = 0.351$) shown in the experimental data

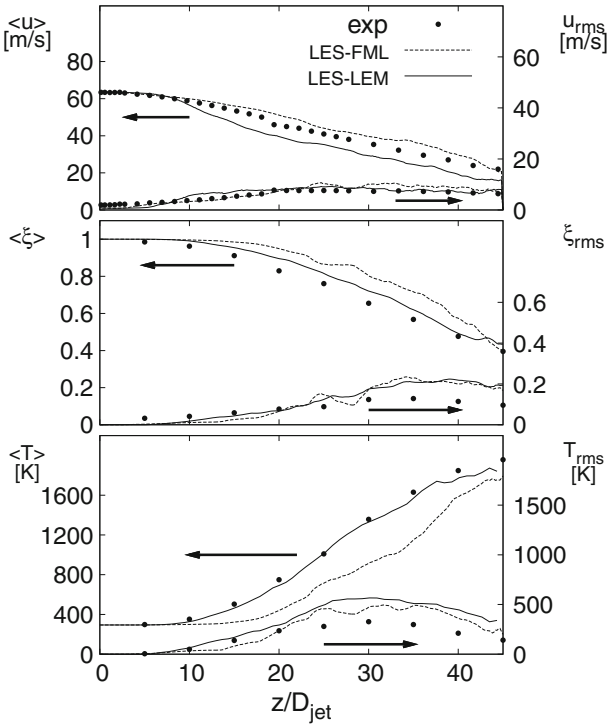

Fig. 5 Profiles of averaged (mean and rms) axial velocity, mixture fraction and temperature along the centerline

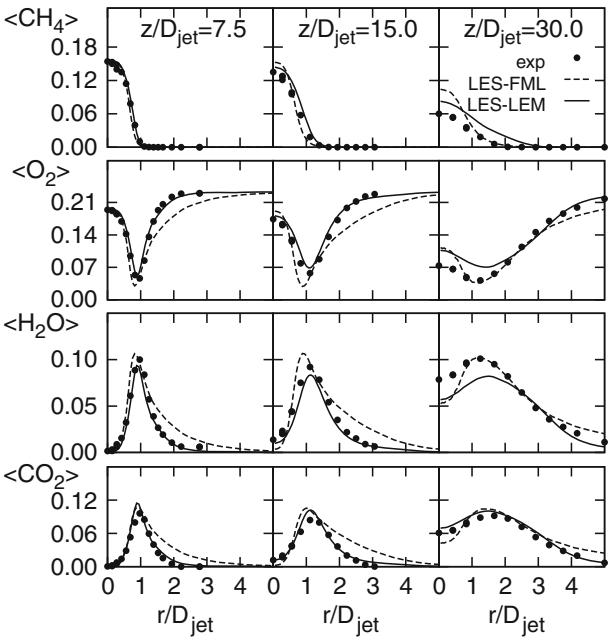

Fig. 6 Radial profiles of mean mass fractions of the chemical species CH_4, O_2, H_2O and CO_2

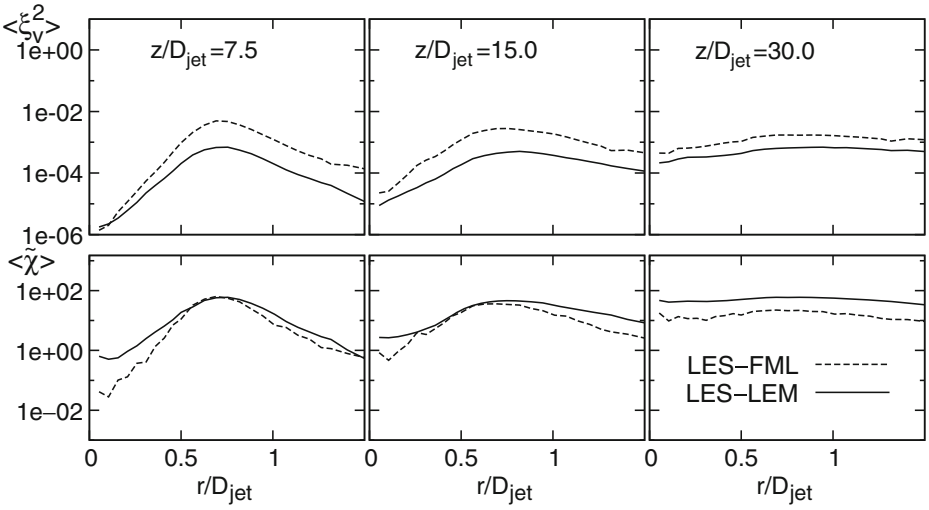

Fig. 7 Radial profiles of mean variance and scalar dissipation rate at several downstream locations

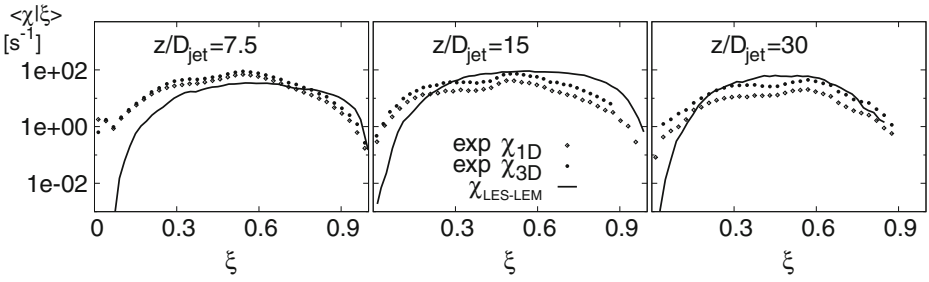

Fig. 8 Radial profiles of the mean conditional scalar dissipation rate

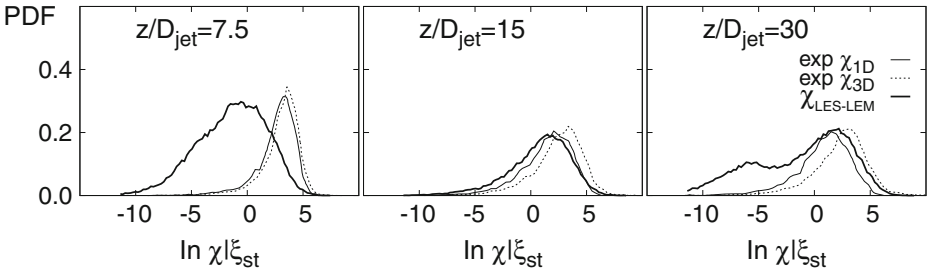

Fig. 9 PDFs of conditional scalar dissipation rate near stoichiometry ($0.33 < \xi < 0.37$))

is not captured by the simulations. This effect is attributed to differential diffusion [20], a phenomenon not considered in this work. Similar agreement is observed in simulations from other groups (see e.g. [10] using a CMC model and [15] with a flamelet-type model).

The Probability Density Functions (PDFs) of the conditional stoichiometric scalar dissipation are shown in Fig. 9. They were formed by restricting the mixture fraction to the interval $0.33 < \xi < 0.37$ and plotted in logarithmic abscissas since the value of χ is broadly distributed in turbulent flames. The experimental shape of the PDF

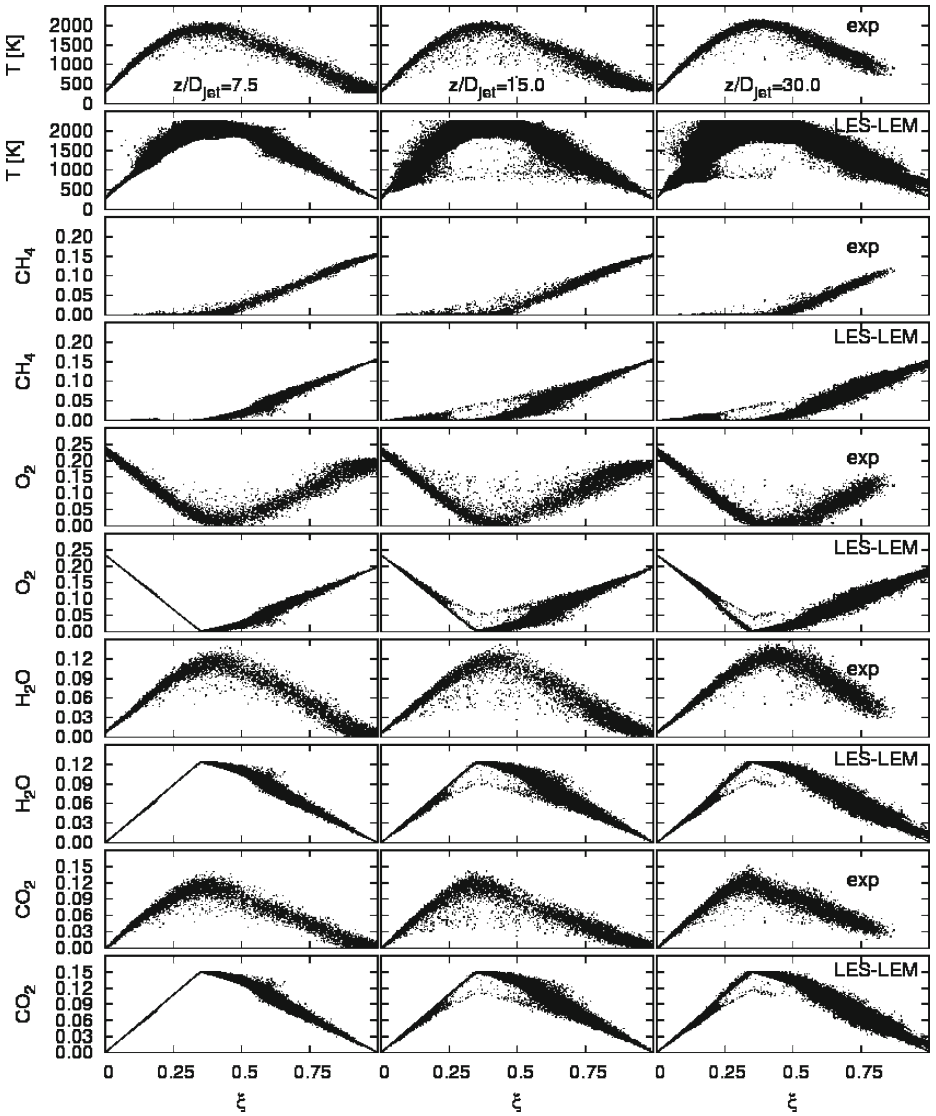

Fig. 10 Scatter plots of experimental and subgrid-LEM distribution of chemical scalars in Flame D

of χ is markedly lognormal. The LES-LEM results show a better agreement with measurements at $z/D_{\text{jet}} = 15$ and 30. The tails at the small values are also present in predictions, although there is a larger bias towards these values for $z/D_{\text{jet}} = 7.5$ and 30. The discrepancies at z/D = 7.5 can be attributed to the intense mixing of the three streams at this early axial station, and its capturing in the scalar, LEM domain. In the paper detailing the experimental work [20], the authors indicate a bias towards low values of scalar dissipation where the gradients of mixture fraction are not accurately captured.

One of the main advantages of the LEM model is its ability to directly incorporate the chemical-reaction term without any modelling assumption since all subgrid scales are resolved by the LEM solver. Scatter plots of subgrid temperature and chemical species versus mixture fraction are shown in Fig. 10. This includes both the experimental and the subgrid-LEM data. The scattering amplitude and, chiefly, the depressed temperature values indicating localized extinction around the stoichiometric value of mixture fraction ($\xi_{st} = 0.351$) are a qualitative indication of the capturing of the turbulence-chemistry interactions at the subgrid level.

As suggested by Karpetis and Barlow [19, 20], the effect of the scalar dissipation on the chemical reaction can be evaluated through doubly conditioned statistics around the stoichiometric values of mixture fraction and scalar dissipation (ξ_{st} and χ_{st}). In Fig. 11, the averaged doubly conditional mass fraction of chemical species are presented. The behaviour shown is consistent with the flamelet theory. The curves are mainly flat for low values of scalar dissipation and change monotonically, increasing or decreasing for reactants or products respectively, as dissipation increases towards eventual extinction. As is noted by Karpetis and Barlow [19], this effect translates to a decrease in the local mixing time ($1/\chi_{st}$) and, therefore, in the Damköler number that leads to the observed behaviour of chemical species.

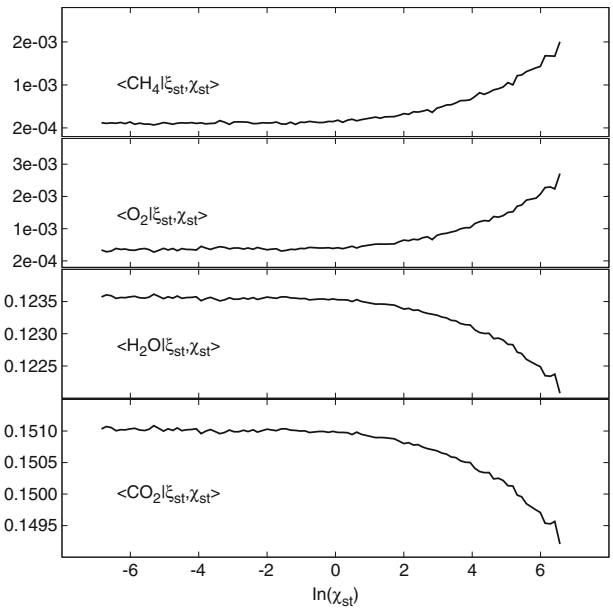

Fig. 11 Average species mass fractions doubly conditioned at the stoichiometric condition

This indicates that although the combustion reaction is represented by a single-step chemical mechanism, the essential nature of the turbulence-chemistry interactions is captured.

5 Conclusions

A subgrid linear eddy mixing and combustion model has been used in the context of LES for modelling a turbulent nonpremixed piloted jet flame (Sandia Flame D). Overall good agreement with measurements was achieved in the prediction of the flame, considering that a simplified one-step chemical mechanism has been employed. The mean and the rms of major flow variables and species have been also compared with conventional flamelet simulations. Although with some discrepancies, the subgrid structure of scalar dissipation rate are in a qualitative agreement with experimental data with reasonably-predicted shapes of the scalar dissipation PDFs. The results show that turbulence-chemistry interactions are represented in the LES-LEM approach, thus highlighting its potential as a prediction tool for turbulent combustion.

Acknowledgements The authors are very grateful to A.N. Karpetis and R.S. Barlow providing the experimental data for scalar dissipation rate. This work was partly funded by the Spanish Ministry for Science and Education under project DPI2003-06551.

References

1. Janicka, J., Sadiki, A.: Large eddy simulation of turbulent combustion system. Proc. Combust. Inst. **30**, 537–547 (2005)
2. Kerstein, A.R.: Linear-eddy modeling of turbulent transport and mixing. Combust. Sci. Technol. **60**, 441–445 (1988)
3. Kerstein, A.R.: Linear-eddy modeling of turbulent transport. part 7: finite-rate chemistry and multi-stream mixing. J. Fluid Mech. **240**, 289–313 (1992)
4. Menon, S., McMurtry, P.A., Kerstein, A.R.: A linear eddy mixing model for large eddy simulation of turbulent combustion. In: Galperin, B., Orszag, S.A. (eds.) Large Eddy Simulation of Complex Engineering and Geophysical Flows, pp. 287–314. Cambidge University Press (1993)
5. McMurtry, P.A., Menon, S., Kerstein, A.R.: A linear eddy sub-grid model for turbulent reacting flows: application to hydrogen-air combustion. Proc. Combust. Inst. **24**, 271–278 (1992)
6. Menon, S., Calhoon, W.: Subgrid mixing and molecular transport modeling for large-eddy simulation of turbulent reacting flows. Proc. Combust. Inst. **26**, 59–66 (1996)
7. Chakravarthy, V.K., Menon, S.: Subgrid modeling of turbulent premixed flames in the flamelet regime. Flow Turbul. Combust. **65**, 133–161 (2000)
8. El-Asrag, H., Menon, S.: Large eddy simulation of bluff-body stabilized swirling non-premixed flames. Proc. Combust. Inst. **31**, 1747–1754 (2006)
9. Barlow, R. (ed.): Proceedings of the TNF Workshop Series: http://www.ca.sandia.gov/tnf (2010). Accessed 25 March 2010
10. Navarro-Martínez, S., Kronenburg, A., Di Mare, F.: Conditional moment closure for large eddy simulations. Flow Turbul. Combust. **75**, 245–274 (2005)
11. Kempf, A., Flemming, F., Janicka, J.: Investigation of lengthscales, scalar dissipation and flame orientation in a piloted diffusion flame by LES. Proc. Combust. Inst. **30**, 557–565 (2005)
12. Vreman, A.W., Albrecht, B.A., van Oijen, J.A., de Goey, L.P.H., Bastiaans, R.J.M.: Premixed and nonpremixed generated manifolds in large-eddy simulation of Sandia Flame D and F. Combust. Flame **153**, 394–416 (2008)
13. Pitsch, H., Steiner, H.: Large eddy simulation of a turbulent piloted methaned/air diffusion flame (Sandia Flame D). Phys. Fluids **12**, 2541–2554 (2000)

14. Pitsch, H.: Improved pollutant predictions in large-eddy simulations of turbulent non-premixed combustion by considering scalar dissipation rate fluctuations. Proc. Combust. Inst. **29**, 1971–1978 (2002)
15. Ihme, M., Pitsch, H.: Prediction of extinction and reignition in nonpremixed turbulent flames using a flamelet/progress variable model: 2. Application in LES of Sandia flames D and E. Combust. Flame **155**, 90–107 (2008)
16. Sheikhi, M.R.H., Drozda, T.G., Givi, P., Jaberi, F.A., Pope, S.B.: Large eddy simulation of a turbulent nonpremixed piloted methane jet flame (Sandia Flame D). Proc. Combust. Inst. **30**, 549–556 (2005)
17. Mustata, R., Valiño, L., Jiménez, C., Jones, W.P., Bondi, S.: A probability density function eulerian monte carlo field method for large eddy simulations: application to a turbulent piloted methane/air diffusion flame (Sandia D). Combust. Flame **145**, 88–104 (2006)
18. Raman, V., Pitsch, H.: A consistent LES/filtered-density function formulation for the simulation of turbulent flames with detailed chemistry. Proc. Combust. Inst. **31**, 1711–1719 (2007)
19. Karpetis, A., Barlow, R.: Measurements of scalar dissipation in a turbulent piloted methane/air jet flame. Proc. Combust. Inst. **29**, 1929–1936 (2002)
20. Karpetis, A., Barlow, R.: Measurements of flame orientation and scalar dissipation in turbulent partially premixed methane flames. Proc. Combust. Inst. **30**, 663–670 (2004)
21. Papadopoulos, C., Sardi, K.: Passive scalar and dissipation simulations with the linear eddy model. In: Kassios, S.C., Langer, C.A., Iacarino, G., Moin, P. (eds.) Complex Effects in Large Eddy Simulations, pp. 191–202. Springer (2007)
22. Kim, W.W., Menon, S., Mongia, H.C.: Numerical simulations of reacting flows in a gas turbine combustor. Combust. Sci. Technol. **143**, 25–62 (1999)
23. Sankaran, V., Menon, S.: Subgrid combustion modeling of 3-D premixed flames in the thin-reaction-zone regimen. Proc. Combust. Inst. **30**, 575–582 (2005)
24. Sankaran, V., Menon, S.: LES of scalar mixing in supersonic mixing layers. Proc. Combust. Inst. **30**, 2835–2842 (2005)
25. Kerstein, A.R.: Linear-eddy modeling of turbulent transport. part 6. Microstructure of diffusive scalar mixing fields. J. Fluid Mech. **231**, 361–394 (1991)
26. Sankaran, V., Menon, S.: Structure of premixed turbulent flames in the thin-reaction-zones regime. Proc. Combust. Inst. **28**, 203–209 (2000)
27. Smith, T.M., Menon, S.: Model simulations of freely propagating turbulent premixed flames. Proc. Combust. Inst. **26**, 299–306 (1996)
28. Fernández-Tarrazo, E., Sánchez, A.L., Liñan, A., Williams, F.A.: A simple one-step chemistry model for partially premixed hydrocarbon combustion. Combust. Flame **147**, 32–38 (2006)
29. Pope, S.B.: Ten questions concerning the large-eddy simulation of turbulent flows. New J. Phys. **6**, 35 (2004)
30. Klein, M., Sadiki, A., Janicka, J.: A digital filter based generation of inflow data for spatially developing direct numerical or large eddy simulations. J. Comput. Phys. **186**, 652–665 (2003)
31. Kempf, A., Klein, M., Janicka, J.: Efficient generation of initial- and inflow-conditions for transient turbulent flows in arbitrary geometries. Flow Turbul. Combust. **74**, 67–84 (2005)
32. CHAM Ltd.: PHOENICS http://www.cham.co.uk/ (2009). Accessed 25 March 2010
33. Gaskell, P.H., Lau, K.C.: Curvature-compensated convective transport: SMART, a new boundedness-preserving transport algorithm. Int. J. Numer. Methods Fluids **8**, 617–641 (1988)
34. Branley, N., Jones, W.P.: Large eddy simulation of a turbulent non-premixed flame. Combust. Flame **127**, 1914–1934 (2001)
35. Steiner, H., Bushe, W.K.: Large eddy simulation of a turbulent reacting jet with conditional source-term estimation. Phys. Fluids **13**, 754–769 (2001)
36. Smooke, M.D., Giovangigli, V.: Formulation of the premixed and nonpremixed test problems. In: Smooke, M.D. (ed.) Reduced Kinetic Mechanism and Asymptotic Approximations for Methane-air Flames, vol. 384 of Lecture Notes in Physics. Springer-Verlag (1991)
37. Ochoa, J.S.: Modelización de la combustión de llamas turbulentas mediante la Simulación de las Grandes Escalas. PhD thesis, Fluid Mechanics Group, University of Zaragoza, Spain (2010, in Spanish)